

LOCAL STABILITY AND GLOBAL INSTABILITY IN IRON-OPAQUE DISKS

MIKOŁAJ GRZĘDZIELSKI, AGNIESZKA JANIUK AND BOŻENA CZERNY

Center for Theoretical Physics, Polish Academy of Sciences, Al. Lotnikow 32/46, 02-668 Warsaw, Poland

(Dated: Received ...; accepted ...)

ABSTRACT

Various processes connected with radiation-matter interaction appearing in hot accretion disk plasma contribute to opacity function κ , given by the Roseland mean. For the case of geometrically thin and optically thick accretion disk, we can estimate the influence of several different components of κ . In the case of high temperatures ($\sim 10^7$) K, the electron Thomson scattering is dominant. At lower temperatures atomic processes become important. The slope $d \log \kappa / d \log T$ can have locally stabilizing or destabilizing effect on the disk. Although the local MHD simulation postulate the stabilizing influence of the atomic processes, only the global time-dependent model can reveal the global disk stability range estimation. This is due to global diffusive nature of that processes.

In this paper, using previously tested GLADIS code with modified prescription of the viscous dissipation, we examine the stabilizing effect of the *iron opacity bump*.

1. INTRODUCTION

The energy output observed in the Galactic X-ray Binaries (XRB), and Active Galactic Nuclei (AGN), suggests that the source of emitted power in these sources must be connected with the gravitational potential energy of a compact object. In most of the former, and all of the latter, this object is a black hole. Its mass can range from a few solar masses, up to a few billion of M_{\odot} . The material that is accreted onto a black hole and emits radiation, may possess substantial angular momentum. In this case, the accretion flow forms a geometrically thin disk, which is located in the equatorial plane of an XRB, or co-aligned with the plane perpendicular to the black hole rotation axis in AGN, if the latter is powered by a Kerr black hole. The classical solution of Shakura & Sunyaev (1973) with their α -viscosity prescription, describes a stationary accretion disk where the dissipated heat is balanced by thermal radiation. As studied by Pringle et al. (1973); Lightman & Eardley (1974) and Shakura & Sunyaev (1976), the viscous stress tensor scaling with a total (i.e., gas plus radiation) pressure leads to the runaway instability of the disk structure. Alternatively, the viscosity prescription may be given by a gas pressure only (in this case the thermal instability does not develop), or by some intermediate law, that invokes a combination of gas and radiation with different weights (see e.g. Szuszkiewicz (1990)). For instance, a general prescription that was recently discussed by Grzedzielski et al. (2016) reads:

$$\tau_{r\phi} = \alpha P_{\text{tot}}^{\mu} P_{\text{gas}}^{1-\mu}. \quad (1)$$

The above model leads to the unstable disk behaviour, which manifests in a limit-cycle type of oscillations of the

emitted luminosity, characteristic for the periodically heated and cooled inner regions of the accretion disk. This kind of cycle is possible, if only the thermal runaway is captured by some stabilizing process. This might be advection of heat onto a black hole, as proposed for the so-called 'slim disk' solution (Abramowicz et al. 1988).

The presence of radiation pressure instability in action of cosmic sources has been a matter of debate (see e.g., review by Blaes (2014)). Nevertheless, there are strong observational hints which support the limit-cycle type of behaviour in at least two well-known microquasars, GRS 1915+105 and IGR J17091-324, in some of their spectral states (Belloni et al. 2000; Altamirano et al. 2011). The limit-cycle oscillations were detected also in the Ultraluminous X-ray source HLX-1, claimed to contain an intermediate-mass black hole (Farrell et al. 2009; Lasota et al. 2011; Servillat et al. 2011; Godet et al. 2012; Wu et al. 2016). Furthermore, some type of non-linear dynamics characteristic for an underlying unstable accretion flow was suggested for a number of other XRBs (Sukova et al. 2015), while the statistical studies of a large sample of sources support the 'reactivation' scenario in the case of compact radio sources hosting supermassive black holes (Czerny et al. 2009).

On the other hand, many of XRBs and AGN seem to be powered by a stable accretion, despite even large accretion rates. Therefore, some stabilizing mechanisms in the accretion process have been invoked, apart from the viscosity prescription itself. For instance, the propagating fluctuations in the flow (Janiuk & Misra 2012) may suppress the thermal instability, or at least delay the development of the instability (Ross et al. 2017).

As recently discussed by Jiang et al. (2016) a possible stabilizing mechanism for the part of an accretion flow might be the opacity changes connected with the ionization of heavy elements. Using the shearing-box simulations of MRI-driven

fluid in the gravitational potential of supermassive black hole (a particular value of black hole mass, $M = 5 \times 10^8 M_\odot$, was used), Jiang et al. (2016) have shown that the flow is stable against the thermal instability, if the opacity includes transitions connected with absorption and scattering on iron ions. This is because the cooling rate, which includes now not only the Thomson scattering (constant) term, but also the absorption and line emission in the Roseland mean opacity, will depend strongly on density and temperature in some specific regions of the disk. In fact, as we discuss below in more detail, the dominant term from opacity changes may completely stabilize the flow locally. The simulations of Jiang et al. (2016) showed that effect but they did not describe the global evolution of the flow, which is the subject of our present work. In our paper we consider the disk stability for the range of black hole masses, characteristic for either XRBs or AGN. We find that the influence of the opacity changes on the global time evolution of the flow is essential, although do not prevent the instability from developing. We show examples of lightcurves produced by our numerical simulation to illustrate this. The paper is organized as follows: in Sect. 2 we present the analytical condition for local thermal instability, in Sect. 3 we present the values of κ opacities for the typical accretion disk densities and temperatures and range of the Iron Opacity Bump, to reveal its influence on global disk behaviour in Sect. 4.

2. LOCAL THERMAL STABILITY IN ACCRETION DISKS

The domination of radiation pressure in the accretion disk leads to the thermal instability (Pringle et al. 1973; Lightman & Eardley 1974; Shakura & Sunyaev 1976; Janiuk et al. 2002). At the instability the heating rate Q_+ grows faster with temperature than cooling rate Q_- . The appearance of local thermal instability is given by the condition:

$$\frac{d \log Q_-}{d \log T} < \frac{d \log Q_+}{d \log T}. \quad (2)$$

The analysis performed in Grzedzielski et al. (2016), under the assumption on constant surface density during thermal timescales leads to following formula on heating rate derivative:

$$\frac{d \log Q_+}{d \log T} = 1 + 7\mu \frac{1 - \beta}{1 + \beta}, \quad (3)$$

where $\beta = P_{\text{gas}}/P$. For the case of this work, we assume $\alpha = 0.02$ and $\mu = 0.56$, being typical for the IMBH and AGN disk case. The radiative cooling rate depends on disk surface density Σ and physical constants Stefan-Boltzmann σ_b and speed of light. The radiative cooling rate is given by following formula (Janiuk et al. 2002; Janiuk et al. 2015; Grzedzielski et al. 2016):

$$Q_- = \frac{4\sigma_b T^4}{3c\Sigma \kappa}. \quad (4)$$

For the radiation pressure dominated disk, combined with Eqs.(2) and (3), from Eq. (4) for $\mu = 0.56$ we get:

$$\frac{d \log Q_-}{d \log T} < 4.92. \quad (5)$$

In our previous papers, only Thomson scattering was assumed, which resulted in the appearance of global radiation pressure instability among all scales of sub-Eddington accretion disks. The recent results of Jiang et al. (2016) are based on stabilizing influence of the iron opacity components. To confront the results of their short time, local 3D MHD shearing-box simulation, we propose the global model, used previously for the case of Intermediate Mass BH HLX-1 accretion disk (Wu et al. 2016; Grzedzielski et al. 2016). According to the lower temperatures in radiation-pressure dominated areas of the accretion disks, we include in our model also the atomic opacity components. Assuming κ being function of ρ and T , we get the formula for log derivative of Q_- :

$$\frac{d \log Q_-}{d \log T} = 4 + \frac{\partial \log \kappa}{\partial \log T} - \frac{4 - 3\beta}{1 + \beta} \frac{\partial \log \kappa}{\partial \log \rho}. \quad (6)$$

The Eq. 6 shows possible stabilizing influence of the negative slope of κ dependent on T and destabilizing influence of the positive slope of κ . Also the dependence on ρ has influence on disk stability. The value of κ itself is not important in the local stability analysis. In case of unstable disk, less efficient cooling being an effect of the greater κ lowers the temperature of unstable equilibrium solution, and enlarge the temperature of stable solution, which can modify the duty cycle quantitatively but not qualitatively. Similarly to Grzedzielski et al. (2016), we can derive the necessary value for the thermal instability:

$$\beta < \frac{7\mu + 3 - \frac{\partial \log \kappa}{\partial \log T} + 4 \frac{\partial \log \kappa}{\partial \log \rho}}{7\mu - 3 + \frac{\partial \log \kappa}{\partial \log T} - 4 \frac{\partial \log \kappa}{\partial \log \rho}} \quad (7)$$

Using the Eqs. (3) and (4), we can define also the thermal stability parameter s :

$$s = \frac{d \log Q_+}{d \log T} - \frac{d \log Q_-}{d \log T} - 3 + 7\mu \frac{1 - \beta}{1 + \beta} - \frac{\partial \log \kappa}{\partial \log T} + \frac{4 - 3\beta}{1 + \beta} \frac{\partial \log \kappa}{\partial \log \rho}. \quad (8)$$

The s parameter is connected with the Lyapunov exponent for the system described by the energy equation in the accretion disk with stress tensor given by Eq. (1). The value $s > 0$ means locally thermally unstable disk, $s \leq 0$ - locally thermally stable. Assuming $\mu = 0.56$ and $\beta \ll 1$ for $\rho = 10^{-8} \text{ g cm}^{-3}$ and $T = 10^5 \text{ K}$ we get $s = -11$ which corresponds to local thermal stability. Nevertheless, for this density the s parameter gains positive values for $T > 3 \times 10^5$, because of radiation pressure domination. Below this temperature, for $T > 1.75 \times 10^5 \text{ K}$, the disk is locally thermally stable because of the negative slope of the bump. For temperatures in the range $1.1 - 1.75 \times 10^5 \text{ K}$, the disk is locally thermally unstable.

3. THE VARIABLE κ - IRON OPACITY BUMP

The opacity κ is the local function describing interaction of high-energy photons with matter from accretion disks. Under the assumptions of local thermal equilibrium, radiation EOS and local vertical hydrostatic equilibrium, both the heating and cooling rates can be described as a function of radius r ,

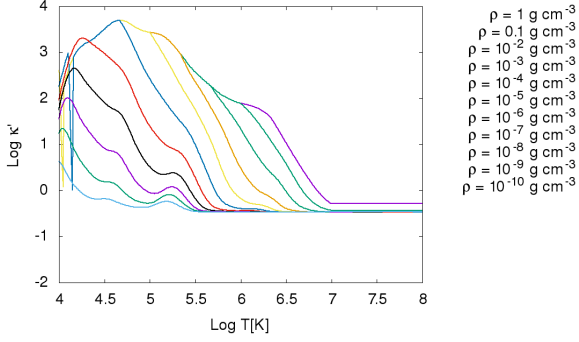


Figure 1. The opacity κ functions including atomic components. The data are taken from (Alexander et al. 1983; Seaton et al. 1994; Różańska et al. 1999).

local density ρ and local temperature T . Although the radius r , affecting the angular momentum transport is important for the heating rate in the α -disk model, it affects the stability analysis only indirectly, via the parameters of stationary solutions. In Fig. 1 we present the profiles of the total opacities for solar metallicity, computed in the function of density and temperature (Alexander et al. 1983; Seaton et al. 1994; Różańska et al. 1999). The combined conditions (3) and (4) to the opacity values results in the significant local stabilization for the temperatures of $1 - 4 \times 10^5$ K and densities about 10^{-8} g cm $^{-3}$ typical for the AGN accretion disks. We fitted the κ function with following formula:

$$\begin{aligned} \kappa &= \kappa_{\text{Th}} + \kappa_{\text{pl}} + \kappa_{\text{bump}} \\ \kappa_{\text{Th}} &= 0.34 \text{cm}^2 \text{g}^{-1} \\ \kappa_{\text{pl}} &= 4.6 \times 10^{23} \rho T^{-3.5} \end{aligned} \quad (8)$$

$$\begin{aligned} \kappa_{\text{bump}} &= 39.8 \rho^{0.2} \left(0.8 \exp - \left(\frac{T - 1.75 \times 10^5 \text{K}}{8.2 \times 10^4 \text{K}} \right)^2 \right. \\ &\quad \left. + 6.3 \exp - \left(\frac{T - 4 \times 10^4 \text{K}}{3 \times 10^4 \text{K}} \right)^2 \right). \end{aligned}$$

The negative stabilizing slope of the iron opacity bump is visible in the Figure 1. In Fig. 2 in the right panel we present the analytical approximation of opacity function from Eq. (1). The detailed results of the dynamical model are presented in Section 4.

4. GLOBAL MODEL

4.1. Values of ρ and T

In Fig. 3 we present typical values of ρ and T for the wide range of accretion disks, computed via the GLADIS code. For the values of ρ and T in the upper left corner, the power law term of κ dominates, but matter with this parameter is too dense and too cold for central areas of sub-Eddington accretion disks. The oblique belt below, presents typical values of ρ and T for the accretion disks with different masses. This area, for $5.1 < \log T < 5.4$ is covered by the Iron Opacity Bump, with stabilizing negative slope (See Sect. 2). According to these results, the stabilizing effect of the negative slope

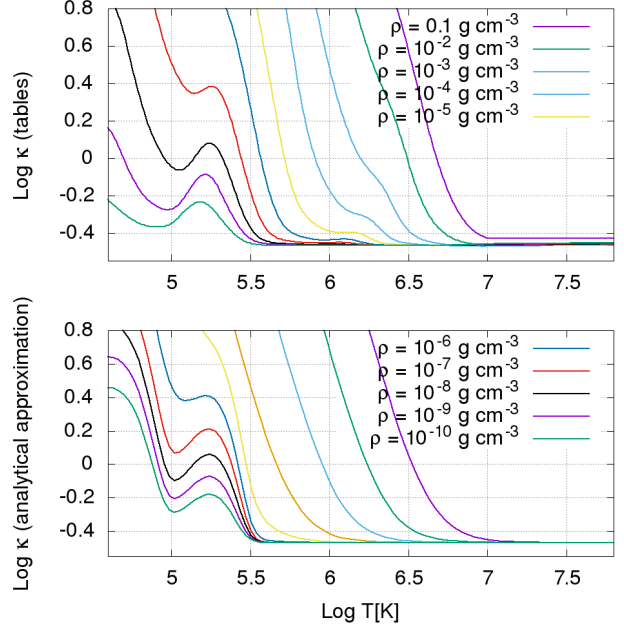


Figure 2. Analytical approximation of the opacity κ functions including atomic components. We model the opacity bump with the Gaussian function

of the iron opacity bump can be visible only for the Active Galactic Nuclei accretion disks with $M \approx 10^8 - 10^9 M_{\odot}$.

4.2. Results for the full model with bump

We perform the model in simulations using the time-dependent global code (Grzedzielski et al. 2016), parameterized with $\alpha = 0.02$, $\mu = 0.56$, and $M = 5 \times 10^8 M_{\odot}$, but now replacing constant Thomson κ with Eq. (1). Similarly to Jiang et al. (2016), we assumed the Eddington rate $\dot{m} = 0.03$. The results of the time-dependent model are presented in Fig. 4. The local shearing-box simulation resulted in the significant stabilization of the disk (Jiang et al. 2016). However, the global model does not confirm these results. The stabilization of the disk, which appears according to local prediction, is not found in general models. Fig. 4 presents the stability parameter profile s defined in Eq. 8. For the inner area of the disk, Thomson component of opacity dominates and temperature is too large to expect any form of stabilization. Outer area of the disk characterize the larger value of total opacity temperature about $1.5 - 2 \times 10^5$ K and negative values of s (the *bump* temperatures). The significant gradient of the s is correlated with the gradient of temperature and gradient of κ in the opposite direction.

The stability parameter, presented in Fig. 4 can reach values between -3 and $-3 + 7\mu$ (0.92 for our choice of μ). In Fig. 4 the typical profile of the s parameter is presented. As the bump is approximately Gaussian function, centered at 1.75×10^5 K, with standard deviation $\sigma = 0.82 \times 10^5$ K, it is expected that the strongest effect of the stabilizing slope would be visible for such temperatures.

The combined outcome of the stabilizing influence of the negative slope of the bump and destabilizing influence of the positive slope of the bump for the dynamical model is presented in Fig. 5. In contradiction to the results of Jiang et al.

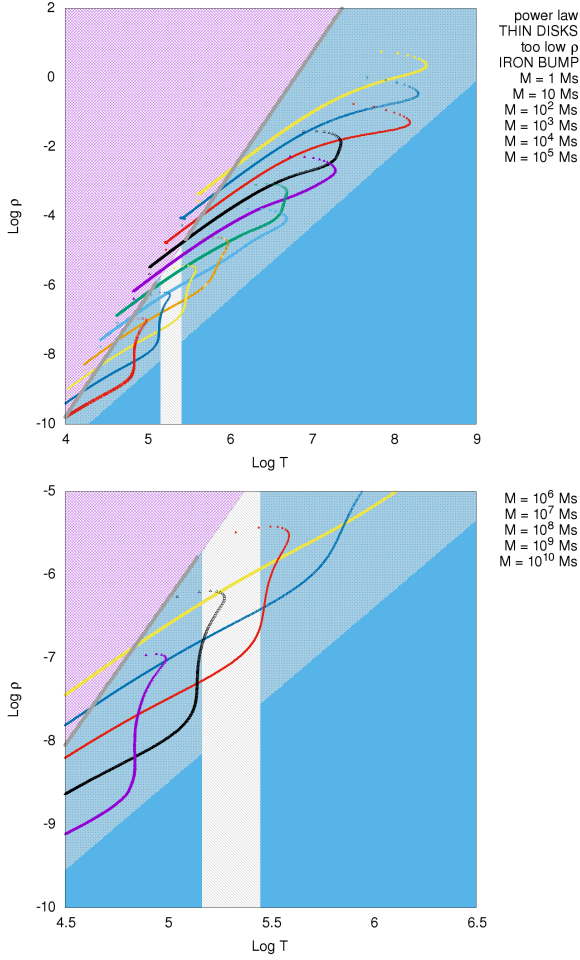


Figure 3. Typical values of the ρ and T for Eddingtonian thin disks for central object mass between 1 and $10^{10} M_{\odot}$. We set $\dot{m} = 0.03$.

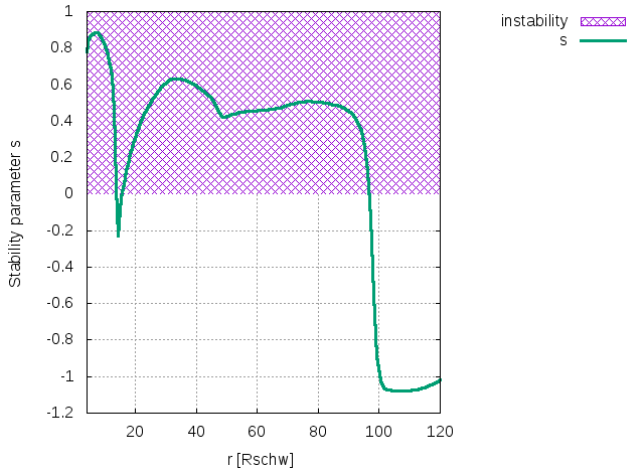


Figure 4. The stability parameter, defined in Eq.(8) during the outburst for $M = 5 \times 10^8 M_{\odot}$, $\dot{m} = 0.03$ (same as in Jiang et al. (2016)).

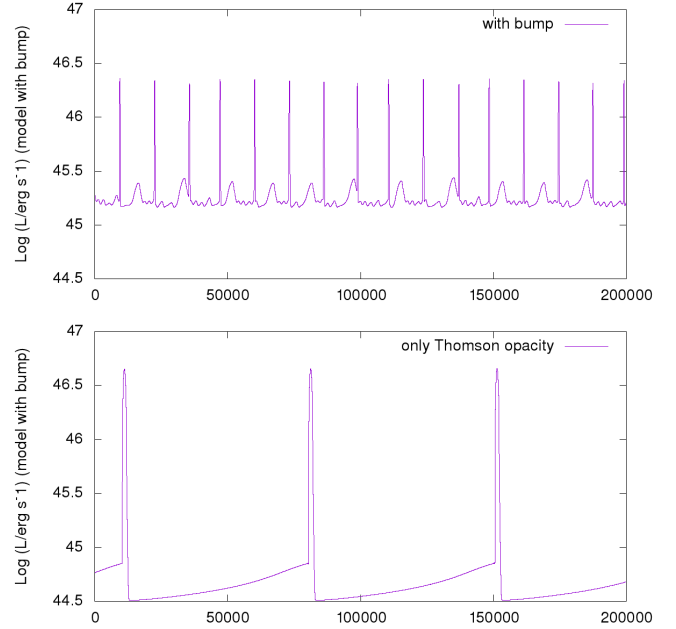


Figure 5. Results of the time-dependent model for $M = 5 \times 10^8 M_{\odot}$, $\dot{m} = 0.03$ (same as in Jiang et al. (2016))

model	amplitude A	period P [yrs]	width Δ
Thomson κ	156	70197	0.0044
bump κ with bump	16.1	12635	0.0023

Table 1. The table describing the flare parameters for the model from Fig. 5 with κ described by formula (1) (second row) and only Thomson κ (third row). Those parameters were described more precisely in (Grzedzielski et al. 2016)

(2016), the iron bump does not stabilize the disk. However, it complicates the lightcurve pattern (many small short flares preceding main outbursts instead of one simple flare), due to the complexity of the photon absorption process, but the inner regions of the disk remains hot enough to perform the limit-cycle oscillations. In effect, the bump partially stabilizes the disk - the amplitude L_{\max}/L_{\min} decreases from 156 for model with constant κ from lower panel of 5 to 16.1 for model with bump (upper panel of 5). The detailed analysis of the lightcurve shape is presented in Table 1.

5. CONCLUSIONS

In our previous paper (Grzedzielski et al. 2016) we computed large grids of models confirming the universality of radiation pressure instability across the BH mass-scale. In this paper we changed the opacity prescription to examine the heavy atoms influence on the accretion disk instability. Comparison between two models presented in Table 1 leads to the conclusions that heavy atoms stabilize the disk partially, but do not imply that the variability vanishes. This stabilizing effect manifests itself rather in a significant period and amplitude decrease, without a relative broadening of the outbursts with respect to their separation. Additionally, some mild *precursors*, being an outcome of a non-monotonic profile of the s parameter distribution, are also visible. That partial stabilization, being an important effect for the Active Galactic Nu-

clei, has only weak influence on the radiation pressure among all BH mass-scale in accretion disk under the assumption of solar metallicity. In case of sources with different metallicity, this effect can change its extent. Finally, we conclude that

the radiation pressure driven limit cycle oscillations, suffering some disturbances from the *iron opacity bump* in case of the AGN disks are also expected, at least for moderately large supermassive black holes ($M = 5 \times 10^8 M_{\odot}$).

REFERENCES

- Abramowicz, M. A., Czerny, B., Lasota, J. P., & Szuszkiewicz, E. 1988, ApJ, 332, 646
- Alexander, D. R., Rypma, R. L., & Johnson, H. R. 1983, ApJ, 272, 773
- Altamirano, D., Belloni, T., Linares, M., et al. 2011, ApJL, 742, L17
- Belloni, T., Klein-Wolt, M., Méndez, M., van der Klis, M., & van Paradijs, J. 2000, A&A, 355, 271
- Blaes, O. 2014, SSRv, 183, 21
- Czerny, B., Siemiginowska, A., Janiuk, A., Nikiel-Wroczyński, B., & Stawarz, Ł. 2009, ApJ, 698, 840
- Farrell, S. A., Webb, N. A., Barret, D., Godet, O., & Rodrigues, J. M. 2009, Nature, 460, 73
- Godet, O., Plazolles, B., Kawaguchi, T., et al. 2012, ApJ, 752, 34
- Grzedzielski, M., Janiuk, A., Czerny, B., & Wu, Q. 2016, ArXiv e-prints
- Janiuk, A., Czerny, B., & Siemiginowska, A. 2002, The Astrophysical Journal, 576, 908
- Janiuk, A., Grzedzielski, M., Capitanio, F., & Bianchi, S. 2015, A&A, 574, A92
- Janiuk, A. & Misra, R. 2012, A&A, 540, A114
- Jiang, Y.-F., Davis, S. W., & Stone, J. M. 2016, ApJ, 827, 10
- Lasota, J.-P., Alexander, T., Dubus, G., et al. 2011, ApJ, 735, 89
- Lightman, A. P. & Eardley, D. M. 1974, ApJL, 187, L1
- Pringle, J. E., Rees, M. J., & Pacholczyk, A. G. 1973, A&A, 29, 179
- Ross, J., Latter, H., & Tehranchi, M. 2017, ArXiv e-prints
- Różańska, A., Czerny, B., Życki, P. T., & Pojmański, G. 1999, MNRAS, 305, 481
- Seaton, M. J., Yan, Y., Mihalas, D., & Pradhan, A. K. 1994, MNRAS, 266, 805
- Servillat, M., Farrell, S. A., Lin, D., et al. 2011, ApJ, 743, 6
- Shakura, N. I. & Sunyaev, R. A. 1973, A&A, 24, 337
- Shakura, N. I. & Sunyaev, R. A. 1976, MNRAS, 175, 613
- Szuszkiewicz, E. 1990, MNRAS, 244, 377
- Wu, Q., Czerny, B., Grzedzielski, M., et al. 2016, ApJ, 833, 79